ATMOSPHERIC LOSS AND VOLATILE FRACTIONATION DURING GIANT IMPACTS. S. T. Stewart, S. J. Lock, and S. Mukhopadhyay. Department of Earth and Planetary Sciences, Harvard University, 20 Oxford Street, Cambridge, MA 02138 (sstewart@eps.harvard.edu).

Introduction: The variations in the elemental and isotopic composition of the atmospheres of terrestrial planets imply a contribution from stochastic differences in their accretion history [1]. Recently, Tucker & Mukhopadhyay [2] argued for multiple partial mantle magma oceans and atmospheric loss events during Earth's accretion based on He/Ne data from the mantle. Although impact events have not typically been considered in studies of chemical fractionation during planet formation, it would be possible to fractionate volatiles that segregate into different physical reservoirs, such as the atmosphere vs. an ocean, if atmospheric loss were a common process [2].

Previous studies of atmospheric blowoff by giant impacts have focused on the 1D mechanics of the loss of a column of atmosphere [3, 4]. Large-scale atmospheric loss occurs when the shock wave imparts a sufficiently high particle velocity around the planet's surface to drive a shock into the atmosphere that ejects a portion of the atmospheric column. Atmospheric loss is more efficient when an ocean is present because the larger particle velocities achieved in the water layer drive a stronger shock in the atmosphere [4]. The surface particle velocities reflect the shock pressure distribution in the target, which is highly sensitive to the impact geometry. Thus, impact-driven atmospheric loss must be considered in 3D.

Here, we derive general scaling laws for blowoff of the atmosphere and ocean during a giant impact and discuss the potential for atmospheric loss and fractionation of volatiles by giant impacts during planet formation.

Impact Calculations: We simulated the propagation of the impact shock through the target and projectile in 3D using the CTH shock physics code [5]. The planets were hydrodynamic and differentiated (30wt% iron core; 70wt% forsterite mantle) with 2000 K potential temperature mantle adiabats. The parameter space spanned planet masses from 0.05 to $0.9M_{Earth}$, six impact parameters b between 0 and 0.93, five mass ratios (M_t/M_p) between 1 and 18, and 6 impact velocities from 1 to $5V_{esc}$. Using Lagrangian tracer particles, we mapped the radial particle velocity on the surfaces of the target and projectile (and also estimated the fraction of mantle melted by the shock).

Using the 1D scaling laws for the loss of a column of atmosphere and ocean from [3, 4], we calculate the loss fraction above each element in the surface map grid for all the impact scenarios. The total atmospheric

and ocean loss fractions are obtained by summing the loss for each grid point weighted by the mapped area.

Blowoff Scaling Laws: Impact fragmentation studies typically scale outcomes by a specific impact energy. Leinhardt & Stewart [6] proposed the form

$$Q_R = 0.5\mu V_i^2 / (M_t + M_p), \qquad (1)$$

where μ is the reduced mass, V_i is the impact velocity, M_t and M_p are the target and projectile masses, respectively. This measure of impact energy does not capture the variations in the shock pressure field that are determined by the impact geometry and projectile-to-target mass ratio. Here, we empirically find that a modified impact energy captures the bulk of the variation in the shock pressure field:

$$Q_S = Q_R (1 + M_p / M_t)(1 - b). \qquad (2)$$

The calculated total atmospheric loss fraction, using the scaling law for a 1:300 atmosphere to ocean mass ratio from [4], is shown in Fig. 1A. Grazing impact events are defined by $b > R_t/(R_t + R_p)$, where R_t and R_p are the radii of the target and projectile [7]. At impact velocities near V_{esc}, grazing collisions hit, separate, and re-impact in graze-and-merge events. Note that atmospheric loss from the second impact is not included in the present analysis. At higher impact velocities, the two bodies hit and escape in hit-and-run events [8]. Non-grazing impacts more efficiently couple the kinetic energy of the projectile to the shock wave in the target, leading to more efficient atmospheric loss.

The atmospheric loss fraction follows a log-linear relationship approaching the specific energy required for total loss (solid line in Fig. 1A). At lower impact energies, atmospheric loss is proportional to the geometric contact area between the two bodies during the early stages of the impact; thus, the dispersion in the grazing data points reflects systematic differences in contact area for different impact geometries. A similar distribution of atmospheric loss is observed for the projectile when the impact energy is defined by reversing the mass ratio in Eq. 2.

In Fig. 1A, the fit to the log-linear region for the ocean loss fraction is shown by the dashed line. The atmospheric loss fraction for targets with no ocean falls slightly above the ocean line.

Volatile Fractionation during Planet Formation: Complete loss of the ocean requires almost an order of magnitude larger impact energies compared to the threshold for total atmospheric blowoff (Fig. 1A).

Thus, there is a decade of specific impact energies between 10^6 and 10^7 J/kg where volatiles in the surface reservoirs of a growing planet may be fractionated by a
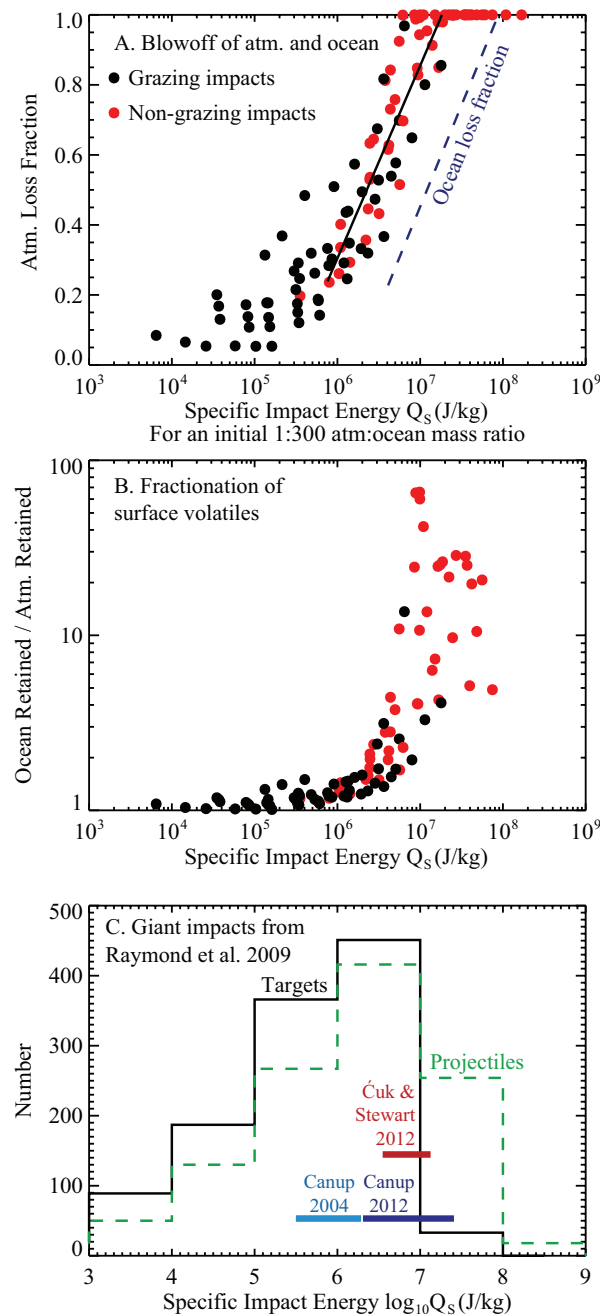
Fig. 1. A. Loss fractions of the atmosphere vs. specific impact energy (points). Solid line is the fit to the loss fraction in the log-linear region. The dashed line is the fit to the ocean loss fraction in the log-linear region. **B.** Fractionation of volatiles in different surface reservoirs vs. impact energy. **C.** Distributions of specific impact energies for all giant impacts from [9]. The impact energy ranges for different Moon-formation scenarios are shown as horizontal bars [10-12].

giant impact (Fig. 1B). The magnitude of fractionation between atmospheric gases (N_2, CO_2) and the ocean (H_2O) is substantial as impact energies approach 10^7 J/kg for the 1:300 atmosphere:ocean case considered here. The giant impact stage of planet formation spans the impact energies required for blowoff of atmospheres and oceans (Fig. 1C). About half of all impact events remove most of the atmosphere of the projectile. Complete atmospheric loss on the larger body is far less frequent and dominated by non-grazing impacts by smaller, faster projectiles.

Based on these results, the cumulative effects of atmospheric blowoff during giant impacts likely contribute to the observed depletion of N and C on the Earth compared to chondrites [2, 13]. Atmospheric loss during the giant impact stage must have acted to varying degrees during the growth of all terrestrial planets. Note that recent high angular momentum Moon formation scenarios [11, 12] would result in substantial atmospheric loss and fractionation of surface volatile reservoirs near the end of Earth accretion (Fig. 1) [see 14].

Conclusions: We have developed general scaling laws to predict the loss fraction of the atmosphere and ocean for any impact scenario. Partial atmospheric blowoff is a frequent process during the giant impact stage of planet formation. The highest energy impact events may remove most of the atmosphere, but rarely blow off the ocean, leading to fractionation of atmophile and hydrophile volatiles on the growing planet. Thus, the stochastic nature of giant impacts leads to variations in the final volatile contents of terrestrial planets.

References: [1] Stewart, S.T. and S. Mukhopadhyay (2013) *LPSC* **44**, Abs. 2419. [2] Tucker, J.M. and S. Mukhopadhyay (in revision) *EPSL*. [3] Genda, H. and Y. Abe (2003) *Icarus* **164**, 149-162. [4] Genda, H. and Y. Abe (2005) *Nature* **433**, 842-844. [5] McGlaun, J.M., et al. (1990) *Int. J. Impact Eng.* **10**, 351-360. [6] Leinhardt, Z.M. and S.T. Stewart (2012) *ApJ* **745**, 79 (27pp). [7] Asphaug, E. (2010) *Chem. Erde* **70**, 199-219. [8] Kokubo, E. and H. Genda (2010) *ApJ Lett.* **714**, L21-L25. [9] Raymond, S.N., et al. (2009) *Icarus* **203**, 644-662. [10] Canup, R.M. (2004) *Icarus* **168**, 433-456. [11] Canup, R.M. (2012) *Science* **338**, 1052-1055. [12] Ćuk, M. and S.T. Stewart (2012) *Science* **338**, 1047-1052. [13] Halliday, A.N. (2013) *GCA* **105**, 146-171. [14] Lock, S.J., et al. (2014) *LPSC* **45**.